Appendix II. Notation

The following symbols are used in this paper:

A = cross-sectional flow area;
a, c = regression coefficient (Table 5)
b = flow width;
D = residue diameter;
F_* = dimensionless shear stress;
g = gravitational acceleration;
P = wetted perimeter;
Q = flow rate;
q = flow rate per unit width;
R = hydraulic radius;
Rn = Reynolds number;
Rn_* = boundary Reynolds number;
S = average slope;
V = mean flow velocity;
V_* = shear velocity;
V_{*c} = critical shear velocity;
y = flow depth;
γ = specific weight of water;
γ_s = specific weight of residue material;
ν = kinematic viscosity;
τ = shear stress; and
τ_c = critical shear stress.

Beginning of Motion for Selected Unanchored Residue Materials

By John E. Gilley[1] and Eugene R. Kottwitz[2]

Abstract: Conservation tillage systems help to maintain residue materials from the previous crop on the soil surface. The potential for serious erosion may exist if crop residues are removed by overland flow. This study is conducted to identify the hydraulic conditions required to initiate residue movement by overland flow. Corn, cotton, peanut, pine needles, sorghum, sunflower, and wheat residue are placed in a flume on smooth and sand surfaces, and flow is then introduced in progressive increments. The discharge rate and flow velocity required to initiate residue movement are identified. Hydraulic measurements are used to calculate the ratio of critical flow depth to residue diameter, critical Reynolds number, critical shear stress, dimensionless shear stress, and boundary Reynolds number. Regression equations are developed to relate dimensionless shear stress to boundary Reynolds number. Close agreement is found between predicted and actual dimensionless shear stress. If residue diameter is known, the regression equations can be used to estimate the beginning of motion for other residue materials. Information obtained in this study can be used to help identify proper residue management practices for conservation tillage systems.

Introduction

Conservation tillage systems leave much of the residue from the previous crop on the soil surface. Crop residue protects the soil surface from raindrop impact, thus reducing soil detachment (Mannering and Meyer 1963). Reduction in overland-flow runoff velocities due to surface residue may also decrease the transport capacity of overland flow. Erosion can be estimated using an inverse, exponential function of percent residue cover (Gilley et al. 1986a, 1986b).

Crop residue creates small ponds in which sedimentation may occur. The volume of water stored in individual impoundments, and corresponding amounts of sedimentation, may be small. However, the cumulative effect of a large number of ponds may be substantial (Brenneman and Laflen 1982).

The presence of crop residues may inhibit rill development. If critical shear stress of the residue material is exceeded and crop residue is removed by overland flow, rill formation may begin. Soil loss usually increases substantially once rills have become established.

A field rainfall-simulation study was conducted by Foster et al. (1982a) to determine critical slope lengths for unanchored cornstalk and wheat straw residue. Foster et al. (1982b) also analyzed the hydraulics of mulch failure. Equations were derived that gave critical discharge rate and critical slope length at which the mulch began to move.

The objective of this study was to identify the hydraulic conditions existing when unanchored residue materials begin to move. Values are provided for

[1]Agric. Engr., USDA-ARS, Univ. of Nebraska, Lincoln, NE 68583-0934.
[2]Res. Engr., Dept. of Biological Systems Engrg., Univ. of Nebraska, Lincoln, NE.

Note. Discussion open until January 1, 1993. To extend the closing date one month, a written request must be filed with the ASCE Manager of Journals. The manuscript for this paper was submitted for review and possible publication on April 1, 1991. This paper is part of the ***Journal of Irrigation and Drainage Engineering***, Vol. 118, No. 4, July/August, 1992. ©ASCE, ISSN 0733-9437/92/0004-0619/$1.00 + $.15 per page. Paper No. 1550.

the ratio of critical flow depth to residue diameter, critical Reynolds number, critical shear stress, dimensionless shear stress, and boundary Reynolds number. Regression equations relating dimensionless shear stress to boundary Reynolds number are also identified.

Hydraulic Equations

The continuity equation for steady flow is defined as

$$Q = VA \quad (1)$$

where Q = flow rate; V = mean flow velocity; and A = cross-sectional flow area. For a rectangular flume, flow depth y is given as

$$y = \frac{Q}{Vb} \quad (2)$$

where b = flow width. In this study, flow depth was determined indirectly using (2) and measurements of Q, V, and b.

Reynolds number, Rn, which is used to describe the ratio of inertial forces to viscous forces, can be expressed as

$$\mathrm{Rn} = \frac{VR}{\nu} \quad (3)$$

where ν = kinematic viscosity; and R = hydraulic radius. Kinematic viscosity can be determined directly from water temperature. The Rn value that causes unanchored residue material to begin to move is defined as critical Rn.

Hydraulic radius R is given as

$$R = \frac{A}{P} \quad (4)$$

where P = wetted perimeter. For a rectangular flume of width b

$$R = \frac{by}{b + 2y} \quad (5)$$

For overland flow conditions where flow width is much greater than flow depth, R can be assumed to be approximately equal to flow depth. For broad-sheet flow conditions

$$\mathrm{Rn} \cong \frac{q}{\nu} \cong \frac{Vy}{\nu} \quad (6)$$

where flow rate per unit width, q, is given as

$$q = \frac{Q}{b} \quad (7)$$

Water flowing over a surface exerts a force on the surface that acts in the direction of flow. This force-per-unit wetted area is called shear stress, τ, and is expressed as

$$\tau = \gamma RS \quad (8)$$

where γ = specific weight of water; and S = average slope. In this study,

critical shear stress, τ_c, is the force-per-unit wetted area required to initiate movement of unanchored residue material.

Shear velocity V_* is defined as

$$V_* = (\mathrm{g}RS)^{1/2} \quad (9)$$

where g = gravitational acceleration. V_* at the threshold condition for residue movement is defined as critical shear velocity V_{*c}.

The submerged weight of the residue material, a lift force, and a drag force may all influence the movement of unanchored residue. Lift and drag forces depend on the same variables, and constants found in theoretical equations are usually determined empirically. Thus, standard procedures used to identify incipient motion usually incorporate lift and drag forces in the analyses. The analytical procedures used in this investigation are similar to those of Shields (Simons and Senturk 1976). However, residue diameter has been used in place of characteristic particle diameter.

The beginning of motion for unanchored residue materials can be identified using dimensionless shear stress, F_* which is defined as

$$F_* = \frac{\tau_c}{(\gamma - \gamma_s)D} \quad (10)$$

where γ_s = specific weight of residue material; and D = residue diameter. The beginning of motion for unanchored residue materials is also a function of the boundary Reynolds number, Rn_*, which is expressed as

$$\mathrm{Rn}_* = \frac{V_{*c}D}{\nu} \quad (11)$$

Rn_* is a dimensionless parameter.

To determine F_* and Rn_*, R must be identified. If roughness coefficient values are known, R can be calculated using the Chézy, Darcy-Weisbach, or Manning equations. The effects of random roughness of the soil surface on hydraulic roughness coefficients were examined by Gilley and Finkner (1991). Hydraulic roughness coefficients for selected residue materials were reported by Gilley et al. (1991). Equations for estimating roughness coefficients for rills and gravel and cobble surfaces have also been identified (Gilley et al. 1990, 1992). For most conditions, rainfall has been found to have a minimal effect on hydraulic resistance (Shen and Li 1973).

Experimental Procedures

The types of residue used in this investigation included corn, cotton, peanut, pine needles, sorghum, sunflower, and wheat. Needles produced by ponderosa pine were included to evaluate conditions existing on forested areas. For each type of residue, 10 randomly selected residue elements were used for characterizing residue dimensions. Mean residue diameter and length and the standard deviation among measurements are shown in Table 1.

Residue length would be expected to be influenced by the type or make of harvesting equipment. Following harvest, residue materials are subjected to weathering and decomposition. The vegetative materials used in this study had all undergone weathering over the winter with the exception of cotton

TABLE 1. Residue Diameter, Residue Length, Density, Residue Rate, Surface Cover, Residue Spacing, and Ratio of Residue Spacing to Residue Diameter of Selected Residue Materials

Residue type (1)	Residue diameter[a] (cm) (2)	Residue length[a] (cm) (3)	Density (kg/m³) (4)	Residue rate (t/ha) (5)	Surface cover (%) (6)	Residue spacing (cm) (7)	Ratio of residue spacing to residue diameter (8)
Corn	1.87 (0.50)	42.9 (14.2)	137	2.0	25	7.5	4.0
Cotton	0.73 (0.26)	36.2 (14.2)	325	2.0	12	6.1	8.3
Peanut	0.36 (0.07)	20.1 (8.3)	365	2.0	17	2.1	5.9
Pine needles	0.12 (0.03)	12.6 (3.5)	383	0.75	30	0.4	3.3
Sorghum	1.59 (0.51)	35.7 (8.3)	137	2.0	22	7.2	4.5
Sunflower	1.93 (0.60)	42.2 (13.0)	124	2.0	15	12.8	6.7
Wheat	0.30 (0.17)	19.4 (10.6)	122	0.25	26	1.2	3.8

[a]Standard deviation of measurements is shown in parentheses.

and peanuts. These two materials were obtained shortly after harvest. No attempt was made to segregate or trim individual residue elements.

Density of the residue materials are also presented in Table 1. To determine density, the residue material was first placed in an oven and dried. The residue material was then removed from the oven and its mass was measured. The residue material was then submerged in water to prevent absorption during the experiment. The volume of residue was identified by placing it in a container of known volume and measuring the quantity of water required to fill the container. Residue mass and volume were then used to calculate density.

All of the residue materials, except pine needles and wheat, were applied at a rate equivalent to 2.0 tonnes/ha. A rate equivalent to 0.75 tonnes/ha was used for pine needles, while wheat straw was applied at a rate equivalent to 0.25 tonnes/ha. Since pine-needle and wheat-residue elements had smaller diameters than the other residue materials, they furnished greater surface cover at a given residue rate.

Surface cover may vary substantially between upland sites. At a particular location, significant differences in residue cover may occur during the year. Surface cover on some upland areas may be much greater than the rates used in this investigation.

The percentage of surface cover provided at a given residue rate was obtained before each test using a photographic grid procedure (Laflen et al. 1978). Residue cover was photographed using 35mm color slide film. The slides were projected onto a screen on which a grid had been superimposed. The number of grid intersections over residue material was determined visually from the projected slides and surface cover was then calculated. Surface cover values for each residue type are shown in Table 1.

Tests were conducted using a flume 0.91-m wide, 7.31-m long, and 0.279-m deep. Water was supplied to the flume using a constant head tank. The slope of the flume was maintained at 1.35%. Since (8) uses slope as an independent variable, values for other slopes can be estimated.

A measured mass of oven-dry residue material was glued randomly onto two sections of reinforced fiberglass sheets each approximately 0.91-m wide and 2.44-m long. The fiberglass sheets with the attached residue were placed in the upper portion of the flume. A measured mass of oven-dry residue material was then placed randomly onto a third fiberglass sheet located in the lower portion of the flume.

The unanchored residue material was placed on two types of surfaces. A relatively smooth fiberglass sheet represented a lower limit for surface roughness. A surface containing sand particles glued onto a fiberglass surface was also used. The diameter of the sand particles varied from 1 mm to 2 mm.

Critical flow rate was determined visually. Flow was introduced in progressive increments until approximately 50% of the unanchored residue material was dislodged. Three replicated tests were run for each residue material on the smooth and sand surfaces to determine critical flow rate. The unanchored residue material was repositioned after the completion of each replicated test. Water temperature was maintained at approximately 21°C throughout the study.

Once critical flow rate had been identified, line sources of fluorescent dye were injected across the flume at downslope distances of 0.91 m and 4.57 m. A fluorometer was used to determine travel time of the dye con-

centration peaks. V was identified by dividing the distance between the two line sources of dye (3.66 m) by the difference in travel time between the two dye concentration peaks. For each critical flow rate, three measurements of flow velocity were made.

Flow Mechanics

When developing theoretical flow concepts, Chow (1959) described isolated-roughness flow. For this flow condition, the roughness elements are so far apart that the wake and vortex at each element are completely developed and dissipated before the flow reaches the next element. Thus, apparent roughness results from form drag on the roughness elements. For isolated-roughness flow, the height of projection of the roughness elements and spacing of elements serve as significant correlating parameters.

Wake-interference flow results when the wake and vortex of closely spaced residue elements interfere with flow conditions in the following element. Finally, quasi-smooth flow occurs when the roughness elements are so close together that the flow essentially skims the crest of the roughness elements.

Information on residue spacing and the ratio of residue spacing to residue diameter could provide insight into the flow process affecting residue movement. Since the residue materials were placed randomly, surface cover information can be used to identify the amount of residue present at a representative cross section. As an example, a 25% surface cover of corn would provide 0.25 m of residue along a representative 1-m cross section. Since mean diameter for corn residue is 1.87 cm, approximately 13 residue elements would be present. For the representative 1-m cross section, average spacing between roughness elements would be approximately 7.5 cm. This would represent a distance of approximately four times the roughness height.

Values for residue spacing and the ratios of residue spacing to residue diameter are shown in Table 1. This information suggests that isolated-roughness flow is the predominate flow condition in this study. Since the height of roughness elements is an important correlating parameter for isolated-roughness flow, use of residue diameter to estimate F_* and Rn_* seems appropriate.

Results

Values for the ratio of critical flow depth to residue diameter, Rn, τ_c, F_*, and Rn_* are provided. Regression equations are presented for estimating the beginning of motion for selected unanchored residue materials. Limitations in the use of the regression equations are also outlined.

Ratio of Critical Flow Depth to Residue Diameter

A critical-flow-depth-to-residue-diameter ratio less than one indicates that the diameter of the residue material is greater than critical flow depth. For both the smooth and sand surfaces (Tables 2 and 3, respectively) critical flow depth was less than the diameter of corn, sorghum, and sunflower residue. Thus, movement of residue material occurred before larger-diameter residue elements became submerged. For each of the residue materials, the ratio of critical flow depth to residue diameter was larger on the sand surface.

Foster et al. (1982a) identified critical flow velocity and critical flow rate per unit width for unanchored corn residue. If broad sheet flow is assumed,

TABLE 2. Ratio of Critical Flow Depth to Residue Diameter, Critical Rn, τ_c, F_* and Rn_* for Selected Residue Materials on Smooth Surface

Residue type (1)	Ratio of critical flow depth to residue diameter (2)	Critical Rn[a] (3)	τ_c (Pa) (4)	F_* ($\times 10^2$) (5)	Rn_* (6)
Corn	0.631	919 (72)	1.55	0.986	765
Cotton	0.836	794 (10)	0.807	1.67	215
Peanut	2.86	1000 (100)	1.36	6.08	138
Pine needles	5.75	540 (41)	0.912	12.6	37.5
Sorghum	0.421	507 (25)	0.888	0.660	490
Sunflower	0.394	895 (58)	1.00	0.606	633
Wheat	1.83	442 (51)	0.723	2.80	83.5

[a]Standard deviation is shown in parentheses.

TABLE 3. Ratio of Critical Flow Depth to Residue Diameter, Critical Rn, τ_c, F_* and Rn_* for Selected Residue Materials on Sand Surface

Residue type (1)	Ratio of critical flow depth to residue diameter (2)	Critical Rn[a] (3)	τ_c (Pa) (4)	F_* ($\times 10^2$) (5)	Rn_* (6)
Corn	0.877	1470 (117)	2.17	1.37	902
Cotton	1.26	1160 (31)	1.22	2.51	263
Peanut	4.50	2210 (44)	2.15	9.57	173
Pine needles	9.67	884 (63)	1.54	21.2	48.7
Sorghum	0.564	884 (11)	1.19	0.885	568
Sunflower	0.523	1030 (12)	1.34	0.808	731
Wheat	3.00	678 (20)	1.19	4.58	107

[a]Standard deviation is shown in parentheses.

these two variables can be used to estimate critical flow depths. Critical flow depths were calculated for two sites examined by Foster et al. (1982a) where corn residue was applied at a rate of 2.2 tonnes/ha. Other residue rates were used, but they were all substantially larger than those examined in this investigation. It can be seen from the ratios of critical flow depth to residue diameter shown in Table 4 that the heights of the corn residue elements were greater than critical flow depth on the Throckmorton and Willer sites.

Critical Reynolds Number

Critical Rn values shown in Tables 2 and 3 can be used to estimate critical flow rates required to initiate residue movement. Values for standard deviation are also given to provide relative estimates of variations between flow measurements. For each of the residue materials, critical Rn was less on the smooth surface.

Data from Foster et al. (1982a) were used to determine critical Rn (Table 4). These critical Rn values were similar to estimates obtained in this study (Tables 2 and 3). Soil surface roughness may affect critical Rn.

TABLE 4. Ratio of Critical Flow Depth to Residue Diameter, Critical Rn, τ_c, F_* and Rn_* for Selected Sites

Location (1)	Ratio of critical flow depth to residue diameter (2)	Critical Rn (3)	τ_c (Pa) (4)	F_* ($\times 10^2$) (5)	Rn_* (6)
Throckmorton	0.123	924	1.59	1.00	929
Willer	0.144	744	2.44	1.54	1152

Note: The hydraulic parameters were calculated from data collected by Foster et al. (1982a) on sites where corn residue was applied at a rate of 2.2 tonnes/ha.

Critical Shear Stress

Forces of static friction act between surfaces at rest with respect to each other. The smallest force necessary to start motion will be the same as the maximum force of static friction. The force per unit area required to initiate movement of unanchored residue material has been defined in this study as τ_c. For each of the residue materials, larger τ_c values were found on the sand surface. This is an expected result of the increased forces of static friction caused by sand particles.

The Throckmorton and Willer sites examined by Foster et al. (1982a) had slopes of 7.00% and 9.27%, respectively. Thus, substantial differences in gradient existed between the laboratory study reported here, which used a flume with a 1.35% slope, and the field investigation of Foster et al. (1982a). However, since slope is included explicitly in the shear stress relationship [(8)], direct comparison of τ values between these two studies is possible. Values for τ_c reported in Table 4 for sites examined by Foster et al. (1982a) were similar to those obtained in this investigation (Tables 2 and 3).

Dimensionless Shear Stress and Boundary Reynolds Number

F_* and Rn_* are shown in Tables 2 and 3. Both values were less on the smooth surface for respective residue materials. F_* can be seen in Fig. 1 to decrease with greater Rn_*.

Close agreement was found between F_* and Rn_* values obtained in this study and those calculated from data of Foster et al. (1982a) (Table 4). Differences in hydraulic parameter values obtained at the Throckmorton and Willer sites could have been influenced by soil surface roughness.

Estimating Beginning of Motion

The F_* and Rn_* data were used to identify the regression equations shown in Table 5. These equations, which were developed for smooth and sand surfaces, relate F_* to a power function of Rn_*. Both regression relations are shown in Fig. 1.

Residue movement can be expected for hydraulic conditions represented by points above the curves shown in Fig. 1. No residue movement occurs for hydraulic conditions characterized by points below the curves. Points on the curves describe conditions suitable for incipient residue movement.

If Rn_* is known, the regression equations shown in Table 5 can be used to solve directly for F_*. Residue diameter is included explicitly in both the F_* and Rn_* relationships. Thus, the regression equations can be used to

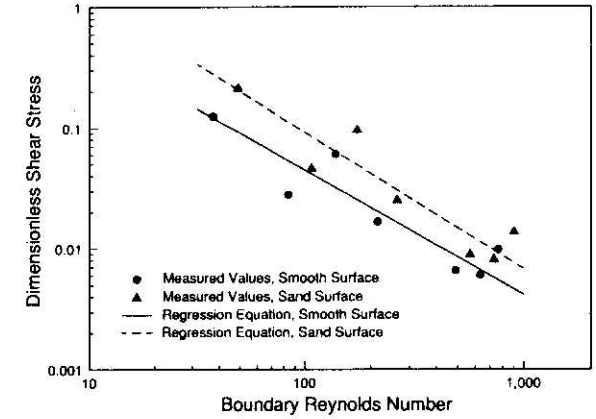

FIG. 1. Dimensionless Shear Stress versus Boundary Reynolds Number for Both Smooth and Sand Surfaces

TABLE 5. Regression Equations for F_* versus Rn_* for Smooth and Sand Surfaces

Surface condition (1)	Regression Coefficients[a] a (2)	c (3)	Coefficient of determination r^2 (4)
Smooth	5.06	−1.03	0.868
Sand	16.7	−1.13	0.886

[a]Regression coefficients a and c are used in the equation $F_* = a(Rn_*)^c$

estimate the beginning of motion for residue materials not included in this study.

The regression equations were used to estimate F_* values shown in Figs. 2 and 3. Close agreement between predicted and actual values were found for both surfaces. Linear regression analysis of predicted versus actual F_* yielded coefficients of determination of 0.868 and 0.886 for the smooth (Fig. 2) and sand surfaces (Fig. 3), respectively.

Limitations of Regression Equations

Unanchored residue materials were used exclusively in this study. Following tillage, a residue element may be partially buried. Other residue materials may be wedged between plants still anchored within the soil, or between gravel and cobble materials. Much larger shear stresses would be required to move partially anchored residue elements.

The effects of grain diameter on τ_c for noncohesive materials were reported by Lane (1953). Detachment and transport of some sand-sized material may occur for values of τ less than those required to initiate residue movement. The detached soil may settle in small ponds created by individual residue elements, providing increased stability to residue materials. Under these conditions, τ_c values much larger than those reported in Tables 2 and 3 would be required to cause residue movement.

The regression equations developed in this study are directly applicable only to isolated-roughness flow conditions where the distance between res-

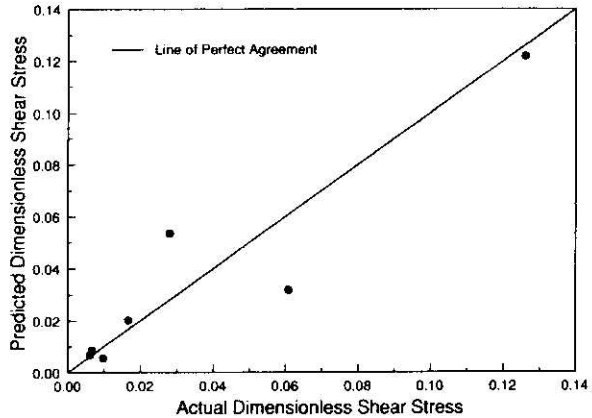

FIG. 2. Predicted versus Actual Dimensionless Shear Stress for Smooth Surface

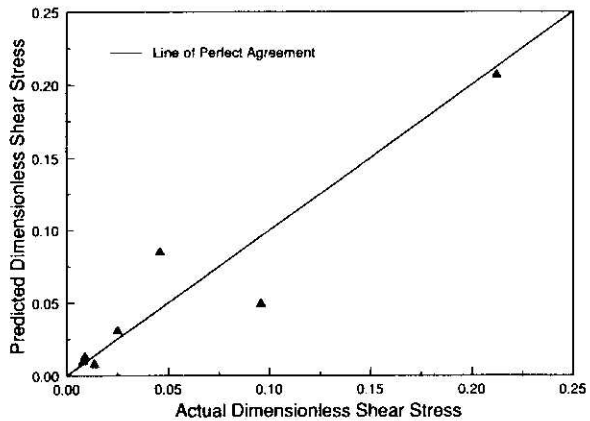

FIG. 3. Predicted versus Actual Dimensionless Shear Stress for Sand Surface

idue elements is significantly greater than residue height. Much different flow conditions may exist for closely spaced residue elements where the wake and vortex produced by a residue element may interfere with flow conditions for the following element. When relatively large residue rates are present, much larger τ values may be required to initiate residue movement.

Summary and Conclusions

Residue materials from the previous crop are maintained on the soil surface with conservation tillage. Relatively small amounts of crop residue may serve to substantially reduce erosion. If crop residues are removed by overland flow, the potential for serious erosion may exist.

Corn, cotton, peanut, pine needles, sorghum, sunflower, and wheat residue were used in this study. The residue materials were placed in a flume on smooth or sand-covered surfaces, and flow was introduced in progressive

increments. The discharge rate and flow velocity required to initiate residue movement were identified.

Hydraulic measurements were used to calculate the ratio of critical flow depth to residue diameter, critical Rn, τ_c, F_*, and Rn_*. Regression equations were developed to relate F_* to Rn_*. Residue diameter is included explicitly in the F_* and Rn_* relationships. Thus, the regression equations can be used to estimate beginning of motion for other residue materials.

The accuracy of the regression equations for estimating F_* was evaluated. Close agreement was found between predicted and actual F_* values. If Rn_* is known or can be estimated, the regression equations can be used to predict F_*. The information developed in this study can be used to identify the hydraulic conditions required to initiate residue movement by overland flow.

Acknowledgment

This paper is a contribution from U.S. Dept. of Agriculture-Agricultural Research Service, Lincoln, Nebraska in cooperation with the Agricultural Research Division, University of Nebraska, also in Lincoln, and is published as journal series number 9521.

Appendix I. References

Brenneman, L. G., and Laflen, J. M. (1982). "Modeling sediment deposition behind corn residue." *Trans. ASAE*, 25(5), 1245–1250.

Chow, V. T. (1959). *Open channel hydraulics*, McGraw-Hill, Inc., New York, N.Y.

Foster, G. R., Johnson, C. B., and Moldenhauer, W. C. (1982a). "Critical slope lengths for unanchored cornstalk and wheat straw residue." *Trans. ASAE*, 25(4), 935–939, 947.

Foster, G. R., Johnson, C. B., and Moldenhauer, W. C. (1982b). "Hydraulics of failure of unanchored cornstalk and wheat straw mulches for erosion control." *Trans. ASAE*, 25(4), 940–947.

Gilley, J. E., Finkner, S. C., Spomer, R. G., and Mielke, L. N. (1986a). "Runoff and erosion as affected by corn residue: Part I. Total losses." *Trans ASAE*, 29(1), 157–160.

Gilley, J. E., Finkner, S. C., and Varvel, G. E. (1986b). "Runoff and erosion as affected by sorghum and soybean residue." *Trans. ASAE*, 29(6), 1605–1610.

Gilley, J. E., Kottwitz, E. R., and Simanton, J. R. (1990). "Hydraulic characteristics of rills." *Trans ASAE*, 33(6), 1900–1906.

Gilley, J. E., and Finkner, S. C. (1991). "Hydraulic roughness coefficients as affected by random roughness." *Trans ASAE*, 34(3), 897–903.

Gilley, J. E., Kottwitz, E. R., and Wieman, G. A. (1991). "Roughness coefficients for selected residue materials." *J. Irrig. Drain. Engrg.*, ASCE, 117(4), 503–514.

Gilley, J. E., Kottwitz, E. R., and Wieman, G. A. (1992). "Darcy-Weisbach roughness coefficients for gravel and cobble surfaces." *J. Irrig. Drain. Engrg.*, ASCE, 118(1), 104–112.

Laflen, J. M., Baker, J. L., Hartwig, R. O., Buchele, W. F., and Johnson, H. P. (1978). "Soil and water loss from conservation tillage systems." *Trans. ASAE*, 21(5), 881–885.

Lane, E. W. (1953). "Design of stable channels." *Trans. ASCE*, 120, 1234–1260.

Mannering, J. V., and Meyer, L. D. (1963). "The effects of various rates of surface mulch on infiltration and erosion." *Soil Sci. Soc. Am. Proc.*, 27(1), 84–86.

Shen, H. W., and Li, R. M. (1973). "Rainfall effect on sheet flow over smooth surface." *J. Hydr. Div.*, ASCE, 99(5), 771–792.

Simons, D. B., and Senturk, F. (1976). *Sediment transport technology*. Water Resources Publications, Fort Collins, Colo.